

## ARTICLE

M.C. Lecomte · G. Nicolas · D. Dhermy · J.C. Pinder  
W.B. Gratzer

## Properties of normal and mutant polypeptide fragments from the dimer self-association sites of human red cell spectrin

Received: 10 August 1998 / Revised version: 13 October 1998 / Accepted: 13 October 1998

**Abstract** We have examined the properties and interactions of expressed polypeptide fragments from the N-terminus of the  $\alpha$ -chain and the C-terminus of the  $\beta$ -chain of human erythroid spectrin. Each polypeptide comprises one complete structural repeating unit, together with the incomplete repeat that interacts with its partner when spectrin tetramers are formed. The shared repeat thus generated is made up of two helices from the C-terminal part of the  $\beta$ -chain and one helix from the N-terminus of the  $\alpha$ -chain. Three mutant  $\beta$ -chain fragments with amino acid substitutions in the incomplete terminal repeat were also studied. The  $\alpha$ - and  $\beta$ -chain fragments were both substantially monomeric, as shown by sedimentation equilibrium. Circular dichroism analysis and thermal denaturation profiles revealed that the complete repeat present in each fragment had entered the stable tertiary fold. Unexpectedly, the conformational stability of the folded  $\beta$ -chain repeat was found to be grossly perturbed by the mutations, all of them well beyond its C-terminal boundary; possible explanations for this phenomenon are considered. Sedimentation equilibrium showed that in equimolar mixtures the wild-type  $\alpha$ - and  $\beta$ -chain peptides formed a 1:1 complex. Mixing curves, observed by circular dichroism, revealed that association was accompanied by an increase in  $\alpha$ -helicity. From continuous-variation profiles an association constant in the range  $1\text{--}2 \times 10^6 \text{ M}^{-1}$  was inferred. The association was unaffected by the apparently unstructured anionic tail of 54 residues, found at the C-terminus of the spectrin  $\beta$ -chain. Of the three mutations in the  $\beta$ -chain fragment, one (an Ala $\rightarrow$ Val replacement in the A helix segment of the incomplete repeat) had a relatively small effect on the association with the  $\alpha$ -chain fragment, whereas Trp $\rightarrow$ Arg mu-

tations in the A and in the remote B helix segments were much more deleterious. These observations are consistent with the relative severities of the haemolytic conditions associated with the mutations.

**Key words** Spectrin · Self-association · Erythrocyte · Hereditary elliptocytosis

### Introduction

The red cell membrane cytoskeleton, on which the mechanical properties of the membrane depend, has the form of a roughly hexagonal lattice composed of spectrin tetramers, extending between junctions made up of short actin filaments and a number of associated proteins (reviewed by Bennett 1990). The spectrin tetramers are formed from two antiparallel  $\alpha\beta$  heterodimers, linked head-to-head. Both spectrin chains consist largely of a series of degenerate repeating units of about 106 residues, each with the conformation of an irregular three-stranded  $\alpha$ -helical coiled-coil (Yan et al. 1993; Pascual et al. 1997). Successive repeats are united by a single long helix, its N-terminal half forming the third helix of one repeat and its C-terminal half the first helix of the next. At the N-terminus of the  $\alpha$ -chain and the C-terminus of the  $\beta$ -chain there are incomplete repeats, comprising one and two strands respectively of the three-helix bundle. It was conjectured that to form a tetramer the spectrin dimers might associate by forming a complete repeat, and there is now compelling evidence that this is indeed the case (DeSilva et al. 1992; Kotula et al. 1993). The  $\beta$ -chain C-terminus also carries a strongly anionic tail of 54 residues, the sequence of which is unrelated to the repeat motif.

The dimer self-association sites are the locus of many mutations, which give rise to hereditary elliptocytosis, a form of haemolytic anaemia with severity varying between mild and lethal (Lux and Palek 1995). In these genetic variants the formation of tetramers is to a greater or lesser degree inhibited and the continuity of the membrane cyto-

M.C. Lecomte · G. Nicolas · D. Dhermy  
INSERM U409, Faculté de Médecine Bichat,  
F-75870 Paris Cedex 18, France

J.C. Pinder · W.B. Gratzer (✉)  
Medical Research Council Muscle and Cell Motility Unit,  
Randall Institute, King's College, 26–29 Drury Lane,  
London WC2B 5RL, UK  
e-mail: wbg@helios.ra.i.kcl.ac.uk

skeletal network is accordingly lost. Wild-type peptides of sufficient length from the N-terminus of the spectrin  $\alpha$ -chain and the C-terminus of the  $\beta$ -chain associate with one another (Kotula et al. 1993; Nicolas et al. 1998). We have expressed such fragments, as well as others with amino acid substitutions in the incomplete C-terminal repeat of the  $\beta$ -chain, found in subjects with hereditary elliptocytosis. Here we examine the conformational characteristics of the fragments and their relation to the association between the  $\alpha$ - and  $\beta$ -chains of normal and the mutant spectrins.

## Materials and methods

### Spectrin fragments

Cloning, expression and purification of the spectrin fragments have been described elsewhere (Nicolas et al. 1998). The following fragments were studied in association assays: (1)  $\alpha_s$  (short  $\alpha$ ), consisting of residues 1–50 of  $\alpha$ -spectrin, comprising the N-terminal C helix; (2)  $\alpha_l$  (long  $\alpha$ ), consisting of residues 1–154 of  $\alpha$ -spectrin, i.e. the N-terminal C helix and the first complete repeat thereafter; (3)  $\beta_s$  (short  $\beta$ ), containing residues 1898–2083, i.e. the incomplete final repeat, consisting of helices A and B, together with the complete preceding repeat; (4)  $\beta_l$  (long  $\beta$ ), comprising residues 1898–2137 and corresponding therefore to  $\beta_s$ , together with the attached anionic C-terminal tail of 54 residues, the sequence of which is unrelated to those of the rod repeats. We examined in addition three mutants of  $\beta_l$ , found in cases of hereditary elliptocytosis, with the substitutions Ala2023→Val, Trp2024→Arg and Trp2061→Arg.

### Sedimentation equilibrium

Sedimentation equilibrium analysis was performed in a Beckman Optima XL-A analytical ultracentrifuge. Solution columns of ca. 2 mm were centrifuged to equilibrium (ca. 28 h) at 10 °C at a rotor speed of 18 000 r.p.m. The solvent was 0.1 M sodium chloride, 20 mM sodium phosphate, pH 7.6. The solution was scanned at 280 nm. The speed was then increased to 42 000 r.p.m. and sedimentation was continued until meniscus depletion had been attained. The solution column was scanned again to determine whether there was any absorbance contribution from non-sedimentable material. Partial specific volumes were calculated from the amino acid compositions. Because of the high state of purity of the preparations, as judged by SDS-polyacrylamide gel electrophoresis, single samples showing evidence of polydispersity were taken to contain only the monomer (of known molecular weight and in all cases the predominant species) and aggregates thereof. To fit the equilibrium distribution the aggregated form was arbitrarily treated as a single component, since in no instance could a satisfactory fit be achieved with an isodesmic model. Equimolar mixtures of  $\alpha$  and  $\beta$  fragments were an-

alysed in the first place with the assumption that three components of known molecular weight (the two monomers and the heterodimer) were the only species present in the system. Thus the equilibrium distribution was fitted to the following equation, assuming ideal solution conditions:

$$A_r = A_{m,\alpha} \exp [M_\alpha(1-\phi_\alpha\rho)\lambda(r^2-r_m^2)] \\ + A_{m,\beta} \exp [M_\beta(1-\phi_\beta\rho)\lambda(r^2-r_m^2)] \\ + K'A_{m,\alpha}A_{m,\beta} \exp[(M_\alpha + M_\beta)(1-\phi_{\alpha\beta}\rho)\lambda(r^2-r_m^2)] + E$$

where  $A_r$  is the protein concentration (in absorbance units) at a distance  $r$  from the centre of rotation and  $A_{m,\alpha}$  and  $A_{m,\beta}$  those of free  $\alpha$  and  $\beta$  monomers at the radius  $r_m$  of the meniscus,  $M_\alpha$  and  $M_\beta$  the molecular weights of the monomers (18 300 and 28 700, respectively) and  $\phi_\alpha$  and  $\phi_\beta$  their partial specific volumes (calculated to be 0.733 and 0.735 ml g<sup>-1</sup>, respectively) and  $\phi_{\alpha\beta}$  that of the complex (taken as 0.734 ml g<sup>-1</sup>);  $\rho$  is the solvent density,  $\lambda \equiv \omega^2/2RT$ , with  $\omega$  the angular velocity,  $R$  the gas constant and  $T$  the absolute temperature, and  $E$  is the non-sedimenting background absorbance, if any, after meniscus depletion.  $K'$  is the association constant in absorbance units of concentration. The molecular weight of the dimer is taken as the sum of those of its constituents.  $K'$  is related to the molar association constant,  $K_a$ , by the factor  $\varepsilon_\alpha\varepsilon_\beta/(\varepsilon_\alpha+\varepsilon_\beta)$ , where  $\varepsilon_\alpha$  and  $\varepsilon_\beta$  are the molar absorptivities of the  $\alpha$  and  $\beta$  monomers, calculated from the amino acid compositions (Perkins 1986), and that of the dimer is taken to be their sum. A closer approximation to the equilibrium mixture takes into account the fraction of aggregated material seen in the equilibrium sedimentation distribution of the  $\beta_l$  fragment by itself. If this is again approximated as a single component with the molecular weight derived from the sedimentation equilibrium of the fragment, a further term can be added to the above equation, of the form  $A_{m,agg} \exp[M_{agg}(1-\phi_\beta\rho)\lambda(r^2-r_m^2)]$ ; here  $M_{agg}$  is the molecular weight of the aggregate and  $A_{m,agg}$  its meniscus concentration, calculated from the proportion inferred to be present.

### Circular dichroism

Circular dichroism (CD) spectra were measured in a Jobin-Yvon CD6 instrument in cells of 0.2–2 mm path-length. For spectra from 185 to 250 nm the solvent was 20 mM sodium phosphate, pH 7.6, but for most purposes the spectra were scanned from 200 to 250 nm in 0.1 M sodium chloride, 20 mM sodium phosphate, pH 7.6. The content of  $\alpha$ -helix was estimated from the molar residue ellipticity at the extremum at 222 nm, taking a value of  $-36\,000$  deg cm<sup>2</sup> dmol<sup>-1</sup> for a fully helical chain (Greenfield and Fasman 1969). Conformations were also analysed by the routine of Provencher and Glöckner (1981). Polypeptide concentrations were determined from absorption spectra, using calculated molar absorptivities as before.

Thermal denaturation profiles were obtained by following the change in ellipticity at 222 nm as a function of temperature. To observe the association between  $\alpha$ - and  $\beta$ -spectrin fragments and establish its stoichiometry, the el-

lipicities of mixtures of varying molar ratios of the two components were measured at constant total molar concentration. Mixtures were left about 30 min to equilibrate and equilibrium was in fact reached in a considerably shorter time. The results were expressed as constant-variation plots (Job plots).

## Results

### Association states of isolated polypeptides

The spectrin fragments used in this study are depicted schematically in Fig. 1. All preparations were pure, as judged by SDS-gel electrophoresis. Onset of turbidity in the solution and loss of material on centrifugation indicated that the short  $\alpha$  fragment,  $\alpha_s$ , comprising only a C helix of the three-helix bundle that characterises the structural repeat, is highly aggregated and polydisperse. In sedimentation equilibrium the large  $\alpha$  fragment,  $\alpha_l$ , by contrast appeared essentially monodisperse (Fig. 2A), with a molecular weight of about 19 700, only slightly higher than the calculated value. Another preparation could best be fitted by including a small fraction of aggregated material. Assuming the theoretical value for the monomer molecular weight, the distribution in this case could be fitted within experimental error by an admixture of 3% by weight of a species of  $M_r$  210 000. At all events, it is clear that the  $\alpha_l$  fragment is very largely monomeric.

The  $\beta$ -chain fragments both gave evidence of some aggregation. Fig. 2B shows the equilibrium distribution of a  $\beta_l$  preparation, used in the mixing experiments depicted below. This cannot be fitted to a single ideal solute distribution. The meniscus molecular weight is close to the calculated value of 28 700, and to fit the entire distribution a single second component was introduced. A good fit is obtained by addition of 17% by weight of a species of molecular weight 83 800 (Fig. 2B). This is necessarily arbitrary,

but establishes the presence (or formation in the course of the sedimentation experiment) in these preparations of aggregates.

It follows from the above results that the single migrating band observed in polyacrylamide gel electrophoresis of the  $\alpha$ - or  $\beta$ -chain fragments in the absence of denaturant (Nicolas et al. 1998) corresponds to the monomer and not to a dimer of the type formed by some folded (Yan et al. 1993; Ralston et al. 1996) or unfolded (MacDonald et al. 1994) spectrin repeats. It further follows that the mutant  $\beta$ -chain fragments (Fig. 1), which migrate identically to the wild-type in electrophoresis, are likewise monomers, rather than dimers.

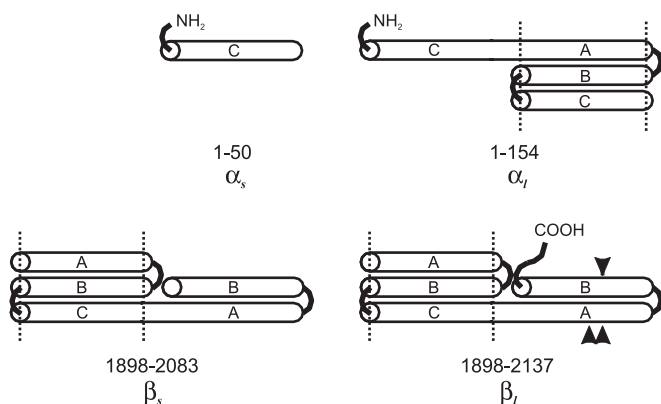


**Fig. 1** Schematic representation of spectrin fragments used in this study. A complete repeat consists of three helices, designated **A**, **B** and **C** (Yan et al. 1993). The  $\alpha$ - and  $\beta$ -chain fragments associate by forming a complete repeat from the incomplete repeats in the two chains

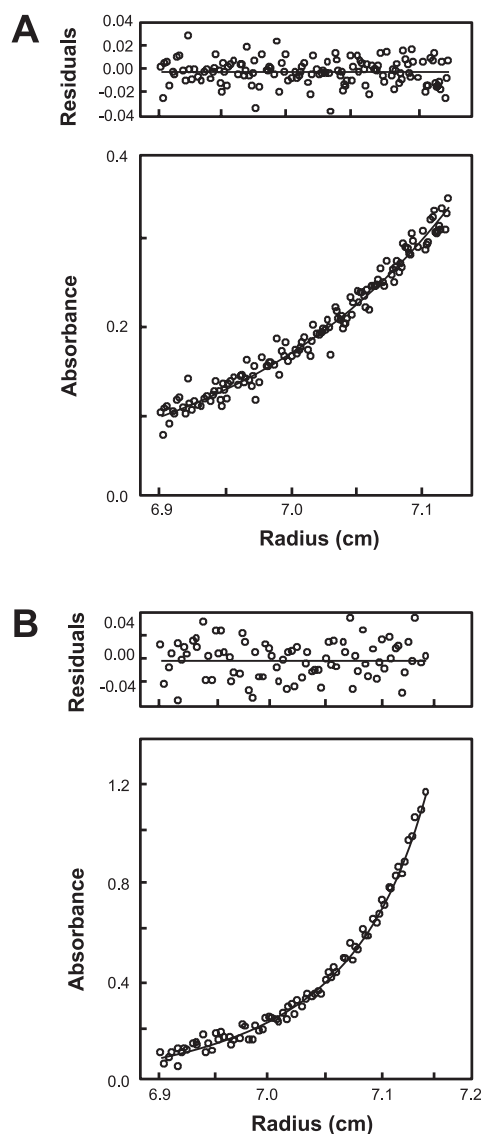


**Fig. 2A, B** Analytical equilibrium sedimentation of **A** the  $\alpha$ -chain fragment,  $\alpha_l$ , showing fit to a monomer of the theoretical molecular weight with 3% by weight of an aggregate of nominal molecular weight 210 000; **B** the  $\beta$ -chain fragment,  $\beta_l$ , showing fit to a monomer of the theoretical molecular weight with 17% of aggregated material of nominal molecular weight, 83 000. Upper panels show the residuals of the calculated fit. See text for conditions

**Table 1** Conformation and stability of spectrin  $\alpha$ - and  $\beta$ -chain fragments

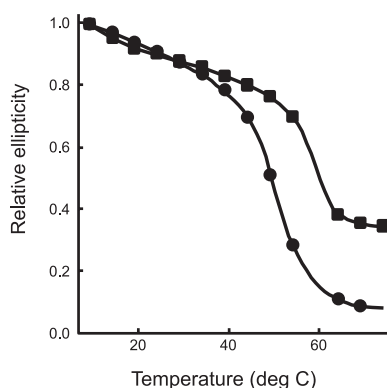
Fragment	$[\theta]_{222}^a$	Percent $\alpha$ -helix <sup>b</sup>	$T_m$ (°C) <sup>c</sup>
$\alpha_i$	-24 300	68	53
$\beta_s$	-22 500	63	60
$\beta_{1wt}$	-19 000	53	62.5
$\beta_1$ Ala2023→Val	-18 100	50	60.5
$\beta_1$ Trp2061→Arg	-17 900	50	57.5
$\beta_1$ Trp2024→Arg	-16 700	46	46.5
$\alpha_s^d$	-1 600	—	—

<sup>a</sup> Molar residue ellipticity at 222 nm (deg cm<sup>2</sup> dmol<sup>-1</sup>) (SEM values are ca.  $\pm 1500$  throughout)

<sup>b</sup> Taking the molar residue ellipticity for a fully  $\alpha$ -helical chain as -36 000 deg cm<sup>2</sup> dmol<sup>-1</sup> (Greenfield and Fasman 1969)

<sup>c</sup> Inflection point of cooperative phase of thermal denaturation profile

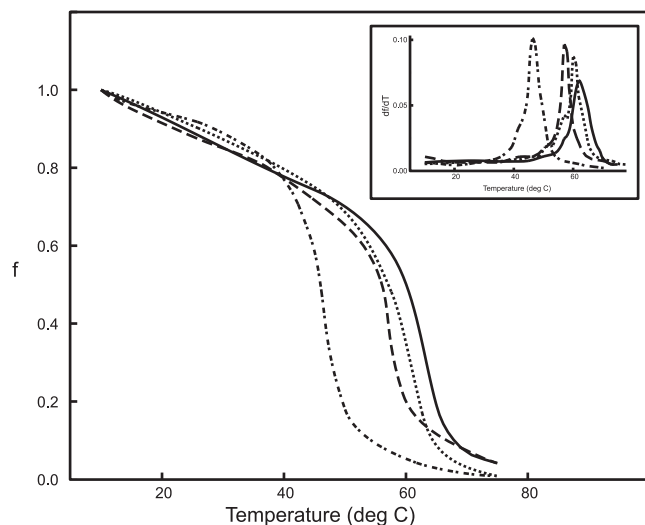
<sup>d</sup> Circular dichroism spectrum shows largely  $\beta$ -sheet structure

**Fig. 3** Thermal denaturation profiles of spectrin  $\alpha$ - and  $\beta$ -chain fragments, measured by the circular dichroism (CD) change at 222 nm:  $\alpha_i$  (●) and  $\beta_s$  (■)

### Conformation and stability of the fragments

Estimates of the  $\alpha$ -helix contents of the fragments, based on the molar residue ellipticity at 222 nm (Greenfield and Fasman 1969) are given in Table 1. Somewhat higher values emerged from the multicomponent analysis of Provencher and Glöckner (1981), but where the  $\alpha$ -helicity is high and  $\beta$ -structure is absent it is unlikely that this procedure is more reliable. For these polypeptides, moreover, as for intact native spectrin, it returned a significant proportion of  $\beta$ -structure and was therefore rejected. The CD spectrum of the short  $\alpha$  fragment,  $\alpha_s$ , was that of a typical  $\beta$ -sheet, which is consistent with the observed aggregated state. All other fragments showed  $\alpha$ -helicity in the range 50–70%. These values are typical of spectrin fragments with incompletely formed tertiary structure (Winograd et al. 1991; Kotula et al. 1993). All three mutant  $\beta_1$  fragments showed degrees of folding that were comparable to or slightly less than that of the wild-type (Table 1).

Figure 3 shows thermal unfolding profiles of the  $\alpha_i$  and  $\beta_s$  fragments, which reveal that both contain a coopera-

**Fig. 4** Thermal denaturation profiles of wild-type and mutant  $\beta_1$  fragments: wild-type (—); Ala(2023)→Val (---); Trp(2024)→Arg (-.-.-); Trp(2061)→Arg (....). The fraction,  $f$ , of the structured state at temperature  $T$  is taken as  $(\theta_T - \theta_U)/(\theta_{10} - \theta_U)$ , where  $\theta_T$ ,  $\theta_{10}$  and  $\theta_U$  represent the ellipticities at 222 nm at  $T$  °C, 10 °C and in the thermally unfolded state. Inset: derivative denaturation profiles (symbols as above)

tively melting structural element, corresponding presumably to the complete repeat present in each. A similar cooperative transition was apparent in the unfolding of a dystrophin repeat, closely resembling those of spectrin (Kahana et al. 1994; Kahana and Gratzner 1995), whereas sequences that did not encompass a complete repeating unit gave broad unfolding profiles with little cooperativity (Kahana and Gratzner 1995). Figure 4 shows a set of denaturation curves for  $\beta_1$  and its three mutants, all of which display similar cooperativity and can therefore be inferred to contain a folded repeat; this is emphasised by the appearance of the derivative plots (Fig. 4, inset). Below the cooperative transition the almost linear fall in ellipticity with increasing temperature can be taken to reflect the progressive unfolding of secondary structure in the incomplete repeat. An unexpected observation, however, was the reduction in thermal stability of the complete repeat engendered by the mutations, all of them outside the repeat boundary. The largest effect, a reduction in the denaturation mid-point of 16 °C, was caused by the Trp2024→Arg substitution.

### Association between $\alpha$ - and $\beta$ -chain fragments

Equilibrium sedimentation of an equimolar mixture of  $\alpha_i$  and  $\beta_1$  fragments showed that these associate with one another (Fig. 5). The molecular weight is close to the calculated value for the dimer of 47 000. A satisfactory fit to the relation for a 1:1 association of two species of molecular weight 18 300 and 28 700 can be obtained; the fit, especially near the bottom of the cell, is improved by including an admixture of unreactive aggregated material in the proportion expected from the sedimentation equilibrium of



the isolated  $\beta$ -chain peptide, but the error minimum is too shallow to allow a definitive evaluation of the equilibrium constant. However, as Fig. 5 shows, the association constant at 10 °C lies between  $10^6$  and  $10^7$  M $^{-1}$ , with a nominal best fit in the range  $2\text{--}4 \times 10^6$  M $^{-1}$ .

Analyses of the association of the  $\alpha_1$  with the  $\beta_s$  and  $\beta_l$  fragments were performed by continuous-variation plots of the CD at 222 nm. An equimolar mixture of  $\alpha_1$  and  $\beta_l$ , for instance, showed an increased ellipticity over the sum of the ellipticities of the monomers which, as Fig. 6 reveals, reflects an increase in  $\alpha$ -helicity, with a concomitant loss of random coil. The small deviation between the experimental and calculated curves in the region of the 208-nm extremum is consistent with the slightly reduced ratio between the ellipticities at 208 and 222 nm characteristic of the coiled-coil state of the  $\alpha$ -helix (Lau et al. 1984; Monera et al. 1996). At the total concentration of the two components in the experiment of Fig. 6 (8.7  $\mu$ M) the increase in helix content was 12–15%, corresponding to some 14–18 residues entering the helical state.

Continuous-variation plots are shown in Fig. 7. The stoichiometry in some experiments deviated perceptibly from equimolar, with an equivalence point closer to a mol fraction of the  $\beta$  fragment of 0.6 than 0.5. This is consistent with the presence of some aggregated chains in the  $\beta$  fragment preparations, as observed in sedimentation equilibrium, which may thus not enter into complexes. The association constant can be estimated from the difference between the observed ellipticity and the value for the fully associated complex. We could not approach this state directly by CD. However, CD data are available for folded single repeats of spectrins (Winograd et al. 1991; Kotula et al. 1993; Menhart et al. 1996; DeSilva et al. 1997; Pantazatos and MacDonald 1997) and the second spectrin-like repeat of human dystrophin, which is highly homologous to the erythroid spectrin repeats (Calvert et al. 1996). These give an average value for the molar residue ellipticity at 222 nm of  $-27\,500 \pm 1600$  deg cm $^2$  dmol $^{-1}$  (six different repeats). [A value shown by MacDonald et al. (1994) is much lower and was omitted]. A comparison with experimental ellipticities at the equivalence point then gives the degree of association and hence an association constant. Within the considerable error of this procedure, our results gave association constants in the range  $1\text{--}2 \times 10^6$  M $^{-1}$ .

A continuous-variation plot with the highly aggregated  $\alpha_s$  fragment showed vestigial interaction with  $\beta_l$ , with only a small increase in ellipticity at 222 nm (not shown). An attempt to overcome the effect of aggregation by mixing the fragments in 6 M guanidinium chloride and dialysing out the denaturant was unsuccessful. Probably therefore a complemented repeating unit needs to be stabilised by folded complete repeats on either side.

The mutant  $\beta_l$  fragments were examined and, in equimolar mixtures with  $\alpha_1$ , the variant Ala2023→Val showed a distinct increase in  $\alpha$ -helicity, smaller by about 40% than that generated by the wild-type fragment at the same concentration. The corresponding association constant is thus lower by a factor of about 5. The remaining mutants, Trp2024→Arg and Trp2061→Arg, by contrast, gave no

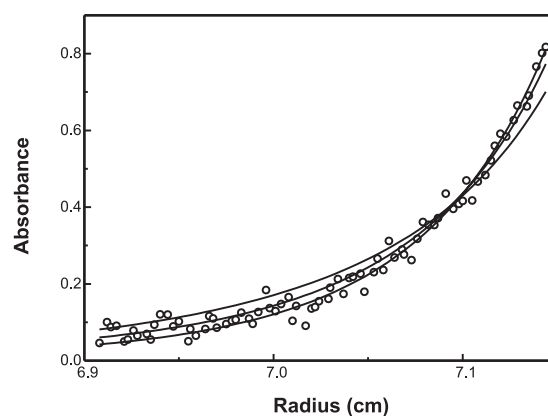


**Fig. 5** Analytical equilibrium sedimentation of a 1:1 mixture of the fragments examined separately in Fig. 2, showing association. The analysis includes the presence of 10% by weight of an aggregated species of nominal molecular weight 84 000 (Fig. 2B), which does not participate in the equilibrium. The curves are calculated for association constants of  $10^5$ ,  $10^6$  and  $10^7$  M $^{-1}$ . The error minimum is too shallow to allow precise determination of the best fit, which lies between  $K_a = 10^6$  and  $10^7$  M $^{-1}$  ( $\chi^2 = 7.4 \times 10^{-4}$  and  $7.1 \times 10^{-4}$ , respectively, and around  $6.4 \times 10^{-4}$  for  $K_a = 2\text{--}4 \times 10^6$  M $^{-1}$ )

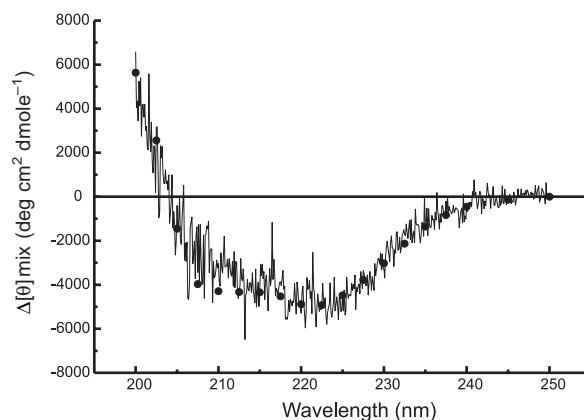


**Fig. 6** CD difference spectrum between an equimolar mixture of  $\alpha_1$  and  $\beta_l$  fragments (at a total concentration of 8.7  $\mu$ M) and the sum of the separate components before mixing. The points are calculated for the transition of 14 residues from random coil to  $\alpha$ -helix

measurable increase in ellipticity on mixing with  $\alpha_1$ , and thus did not enter into a complex to any extent discernible by this technique in this concentration range.

## Discussion

The CD spectra, together with the thermal unfolding profiles, show that the complete repeat, present in both the  $\alpha$ - and  $\beta$ -chain fragments, entered the stable tertiary fold. This is to be expected on the basis of earlier data. Moreover, because the first turn of the  $\alpha$ -helix of a repeat packs into the three-helix bundle constituting the contiguous preceding repeat (Yan et al. 1993; Cross et al. 1990), an extension of

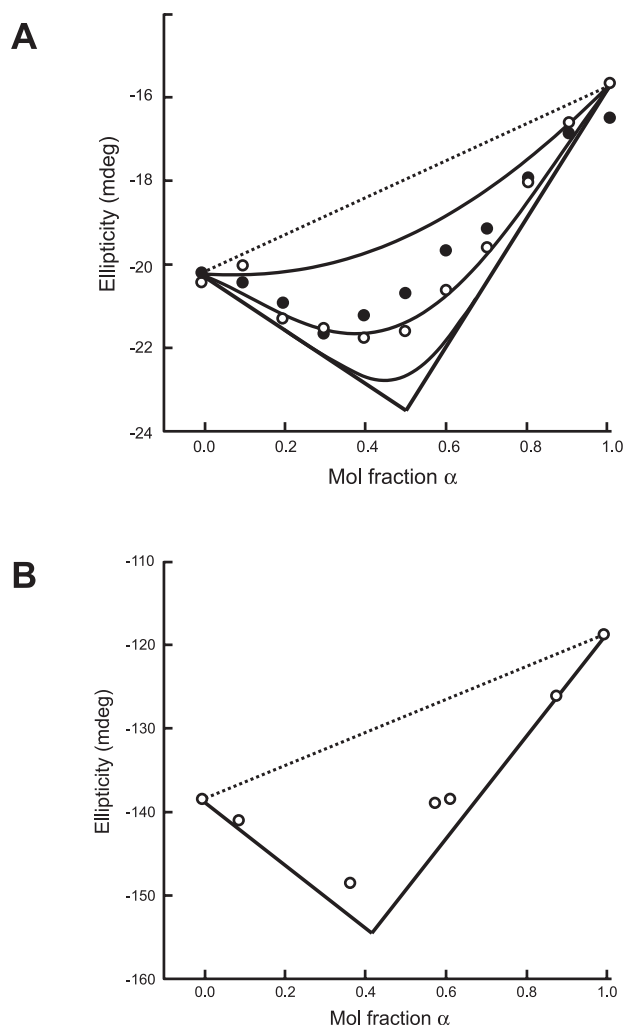


**Fig. 7A, B** Continuous-variation plots. **A** Complex formation between  $\alpha_1$  and  $\beta_1$  spectrin fragments at  $8.7 \mu\text{M}$  at  $10^\circ\text{C}$  ( $\circ$ ) and  $20^\circ\text{C}$  ( $\bullet$ ). *Full straight lines* represent mixing with 100% complex formation (infinite association constant) and *broken lines* mixing with no complex formation. The curves are calculated for association constants (*top to bottom*) of  $10^5$ ,  $10^6$  and  $10^7 \text{ M}^{-1}$ . **B** Complex formation between  $\alpha_1$  and  $\beta_2$  fragments at  $66 \mu\text{M}$  and  $10^\circ\text{C}$  ( $\circ$ )

the sequence by some residues on the C-terminal side increases the stability of the structure significantly (Calvert et al. 1996). The same explanation probably applies to the elevated stability of two contiguous spectrin repeats, relative to an isolated repeat (Menhart et al. 1996).

The large influence on conformational stability of an amino acid replacement far from the C-terminal boundary of the complete repeat (Fig. 1) is entirely unexpected, on the other hand. An estimate of the effects of the mutations on the folding free energy can be made. Becktel and Schellman (1987) have shown that for a relatively small perturbation of thermal stability by a mutation the free energy change,  $\delta(\Delta G)$ , can be determined without knowledge of  $\Delta C_p$ . This depends on the fact that over a sufficiently narrow temperature range the curves relating Gibbs free energy to temperature lie nearly enough parallel. It then fol-

lows that  $\delta(\Delta G) = \Delta T_m(\Delta H(\text{wt})/T_m(\text{wt}))$ , where  $T_m$  is the denaturation mid-point, at which  $\Delta G = 0$ ,  $\Delta T_m$  the change in  $T_m$  caused by the mutation, and  $\Delta H(\text{wt})$  and  $T_m(\text{wt})$  the enthalpy of unfolding and the denaturation mid-point respectively of the wild-type protein.  $\Delta H(\text{wt})$  can be determined from a van't Hoff plot over the denaturation range. For this purpose the equilibrium constant for unfolding is found at each temperature from the ratio of the integrated areas of the derivative curves (Fig. 4, inset) above and below that temperature, i.e.

$$K = \int_0^T (d\theta/dT) dT / \int_T^\infty (d\theta/dT) dT.$$

The resulting van't Hoff plots (not shown) were linear within experimental error, except in the case of the mutant Ala2023→Val, which showed some curvature towards lower temperatures; they gave standard enthalpies in the range 29–32 kcal mol<sup>-1</sup>. The reductions in folding free energies at  $T_m(\text{wt})$  relative to the wild-type polypeptide were 0.5, 1.4 and 0.2 kcal mol<sup>-1</sup> for mutants Trp2061→Arg, Trp2024→Arg and Ala2023→Val, respectively.

The effect of mutations outside the folding unit on the stability of its tertiary structure in the fragment is the more unexpected because the mutated residues are in a largely unstructured appendage. A possible basis for the effect is that the unfolded state is stabilised by intra-chain interactions, rather than that the folded state is destabilised by weakened interactions. However, there is evidence that, in the native state of the spectrin rod, cooperativity may prevail over large distances, for the association between dimers is impaired by mutations up to eight repeats removed from the association site. (Data are summarised by Lux and Palek 1995.) It is also possible that in the spectrin dimer a local perturbation of the rod conformation disrupts the lateral association of the  $\alpha$ - and  $\beta$ -chains, so that the excluded volume available to the association sites at the chain ends is increased. The melting profiles of the fragments (Fig. 4), especially of mutant Trp2024→Arg, suggest at all events that such mutations could cause partial unfolding of the critical region of the rod domain at physiological temperature. Such an effect could lead to a change in the elastomeric properties of the spectrin tetramer or its partial dissociation into dimers, as indicated.

The helical segments of incomplete repeats are clearly partly or largely in the randomly coiled conformation until they associate with their complementary partial repeat. The increase in  $\alpha$ -helicity on association of the  $\alpha$ - and  $\beta$ -chain fragments allowed us to follow the formation of 1:1 complexes. The long and short  $\beta$ -chain fragments behaved indistinguishably from one another, showing that the anionic C-terminal tail of the  $\beta$ -chain neither participates in nor weakens the association of spectrin dimers to tetramers. Comparison of the measured helicities of the long and the short  $\beta$ -chain fragment indicates that this segment is unstructured. Its function remains unclear.

Our results confirm that terminal fragments of the spectrin  $\alpha$ - and  $\beta$ -chains will associate with each other in a 1:1 complex, in a manner analogous to the self-association of intact spectrin heterodimers. This agrees with the results

of Speicher and co-workers (DeSilva et al. 1992; Kotula et al. 1993) and our own recent data (Nicolas et al. 1998). The association is rapid, without the large activation energy that characterises the dimer-tetramer equilibrium of intact spectrin. The estimated association constants are within the range reported in the earlier study, based on gel electrophoretic analysis (Nicolas et al. 1998), which depends on separation of the associated from the unassociated chains. The interacting fragments are themselves monomeric (but for some aggregated material, especially in the  $\beta$  fragment preparations), and do not form the homodimers observed by Yan et al. (1993) and Ralston et al. (1996) to be generated by a repeat of *Drosophila* spectrin. Correctly phased and folded single repeats of spectrin (MacDonald et al. 1994; Pascual et al. 1996; DeSilva et al. 1997) and of dystrophin (Calvert et al. 1996) were also monomeric. MacDonald et al. (1994) found, however, that two chicken brain spectrin repeats, which were not in the correct phasing and were therefore not folded, formed dimers or trimers in solution. The incomplete repeat elements, present in addition to the folded repeat in our fragments, did not induce such self-association.

The  $\beta$ -chain mutations all reduced the extent of association with the  $\alpha$ -chain fragment, as observed before (Nicolas et al. 1998). The effect was least for mutation Ala2023→Val, with a diminution in negative free energy of heterodimer formation at 10 °C of ca. 1 kcal mol<sup>-1</sup> relative to the wild-type peptide (corresponding to an approximately fivefold reduction in association constant). The relative destabilisation of the heterodimer engendered by the mutations is consistent with the fraction of spectrin dimer present in the cells of the affected patients and with the severity of the haemolytic condition. Thus the mutations Trp2061→Arg and Trp2024→Arg cause elliptocytosis with a significant haemolytic anaemia, while the substitution Ala2023→Val gives rise to half the amount of dimer caused by the other two mutations and an asymptomatic elliptocytosis (Parquet et al. 1994; Glele-kakai et al. 1996).

Trp2024 is highly conserved throughout the spectrin superfamily. Its position in the structure (Yan et al. 1993) gives little indication of its function, but its replacement even by phenylalanine has a considerable effect on the stability of the fold (Pantazatos and MacDonald 1997). Examination of the crystal structure led to the inference that the insertion of arginine in this position (residue 17 in the A helix) could introduce a repulsion between the cationic charge and that of the arginine at B21 (Pascual et al. 1997). The replacement of Ala2023 by valine (residue A18) should have no effect on any interactions in the tertiary fold, since this residue lies on the outside of the helix bundle. In the third mutant, Trp2061 at B18 is replaced in position d of the heptad hydrophobic repeat by arginine. An inspection of the model reveals no obvious unfavourable interactions, and in fact the same position is occupied by charged residues [histidine in the peptide studied by Yan et al. (1993)] in many of the spectrin repeats. Several aspects of the structure-stability relations in spectrin and its analogues thus remain unresolved.

**Acknowledgements** We are grateful to the British Council and the Alliance Française for support under the Alliance project scheme.

## References

- Becktel WJ, Schellman JA (1987) Protein stability curves. *Biopolymers* 26: 1859–1877
- Bennett V (1990) Spectrin-based membrane skeleton – a multipotential adapter between plasma-membrane and cytoplasm. *Physiol Rev* 70: 1029–1065
- Calvert R, Kahana E, Gratzer WB (1996) Stability of the dystrophin rod domain fold: evidence for nested repeating units. *Biophys J* 71: 1605–1610
- Cross RA, Stewart M, Kendrick-Jones J (1990) Structural predictions for the central domain of dystrophin. *FEBS Lett* 262: 87–92
- DeSilva TM, Peng K-C, Speicher KD, Speicher DW (1992) Analysis of human red cell spectrin tetramer (head-to-head) assembly using complementary univalent peptides. *Biochemistry* 31: 10872–10878
- DeSilva TM, Harper SL, Kotula L, Hensley P, Curtis PJ, Otvos L, Speicher DW (1997) Physical properties of a single-motif erythrocyte spectrin peptide: a highly stable independently folded unit. *Biochemistry* 36: 3991–3997
- Glele-kakai C, Garbarz M, Lecomte MC, Leborgne S, Galand C, Bournier O, Devaux I, Gautero H, Zohoun I, Gallagher PG, Forget BG, Dhermy D (1996) Epidemiologic studies of spectrin mutants related to hereditary elliptocytosis and spectrin polymorphisms in Benin. *Br J Haematol* 95: 57–66
- Greenfield N, Fasman GD (1969) Computed circular dichroism spectra for the evaluation of protein conformation. *Biochemistry* 8: 4108–4116
- Kahana E, Gratzer WB (1995) Minimum folding unit of dystrophin rod domain. *Biochemistry* 34: 8110–8114
- Kahana E, Marsh PJ, Henry AJ, Way M, Gratzer WB (1994) Conformation and phasing of dystrophin structural repeats. *J Mol Biol* 235: 1271–1277
- Kotula L, DeSilva TM, Speicher DW, Curtis PJ (1993) Functional characterization of recombinant human red cell  $\alpha$ -spectrin polypeptides containing the tetramer binding site. *J Biol Chem* 268: 14788–14793
- Lau SYM, Taneja AK, Hodges RS (1984) Synthesis of a model protein of defined secondary and quaternary structure. Effect of chain length on the stabilization and formation of two-stranded  $\alpha$ -helical coiled coils. *J Biol Chem* 259: 13253–13261
- Lux SE, Palek J (1995) In: Handin RI, Lux SE, Stossel TP (eds) *Blood: principles and practice of hematology*. Lippincott, Philadelphia, pp 1701–1818
- MacDonald RI, Musacchio A, Holmgren RA, Saraste M (1994) Invariant tryptophan at a shielded site promotes folding of the conformational unit of spectrin. *Proc Natl Acad Sci USA* 91: 1299–1303
- Menhart N, Mitchell T, Lusitani D, Tapouzien N, Fung LW-M (1996) Peptides with more than one 106-amino acid sequence motif are needed to mimic the structural stability of spectrin. *J Biol Chem* 271: 30410–30416
- Monera OD, Sönnichsen FD, Hicks L, Kay CM, Hodges RS (1996) The relative positions of alanine residues in the hydrophobic core control the formation of two-stranded or four-stranded  $\alpha$ -helical coiled-coils. *Protein Eng* 9: 353–363
- Nicolas G, Pedroni S, Fournier C, Gautero H, Craescu G, Dhermy D, Lecomte MC (1998) The spectrin self-association site: characterization and study of  $\beta$ -spectrin mutations associated with hereditary elliptocytosis. *Biochem J* 332: 81–89
- Pantazatos DP, MacDonald RI (1997) Site-directed mutagenesis of either the highly conserved Trp-22 or the moderately conserved Trp-95 to a large hydrophobic residue reduces the thermodynamic stability of a spectrin repeating unit. *J Biol Chem* 272: 21052–21059

- Parquet N, Devaux I, Boulanger L, Galand C, Boivin P, Lecomte MC, Dhermy D, Garbarz M (1994) Identification of three novel spectrin  $\alpha$ /74 mutations in hereditary elliptocytosis: further support for a triple-stranded folding unit model of the spectrin heterodimer contact site. *Blood* 84: 303–308
- Pascual J, Pfuhl M, Rivas G, Pastore A, Saraste M (1996) The spectrin repeat folds into a three-helix bundle in solution. *FEBS Lett* 383: 201–207
- Pascual J, Pfuhl M, Walther D, Saraste M, Nilgas M (1997) Solution structure of the spectrin repeat: a left-handed antiparallel triple-helical coiled-coil. *J Mol Biol* 273: 740–751
- Perkins SJ (1986) Protein volumes and hydration effects. The calculation of partial specific volumes, neutron scattering matchpoints and 280-nm absorption coefficients for proteins and glycoproteins from amino acid sequences. *Eur J Biochem* 158: 169–180
- Provencher SW, Glöckner J (1981) Estimation of globular protein secondary structure from circular dichroism. *Biochemistry* 20: 33–37
- Ralston GB, Cronin TJ, Branton D (1996) Self-association of spectrin repeating segments. *Biochemistry* 35: 5257–5263
- Winograd E, Hume D, Branton D (1991) Phasing the conformational unit of spectrin. *Proc Natl Acad Sci USA* 88: 10788–10791
- Yan Y, Winograd E, Viel A, Cronin T, Harrison SC, Branton D (1993) Crystal structure of repetitive unit of spectrin. *Science* 262: 2027–2030